npg

ORIGINAL ARTICLE

The effect of nutrients on carbon and nitrogen fixation by the UCYN-A–haptophyte symbiosis

Andreas Krupke[1,3], Wiebke Mohr[2,4], Julie LaRoche[2,5], Bernhard M Fuchs[1], Rudolf I Amann[1] and Marcel MM Kuypers[1]

[1]*Max Planck Institute for Marine Microbiology, Bremen, Germany* and [2]*Helmholtz-Zentrum für Ozeanforschung, Kiel, Germany*

Symbiotic relationships between phytoplankton and N_2-fixing microorganisms play a crucial role in marine ecosystems. The abundant and widespread unicellular cyanobacteria group A (UCYN-A) has recently been found to live symbiotically with a haptophyte. Here, we investigated the effect of nitrogen (N), phosphorus (P), iron (Fe) and Saharan dust additions on nitrogen (N_2) fixation and primary production by the UCYN-A–haptophyte association in the subtropical eastern North Atlantic Ocean using *nifH* expression analysis and stable isotope incubations combined with single-cell measurements. N_2 fixation by UCYN-A was stimulated by the addition of Fe and Saharan dust, although this was not reflected in the *nifH* expression. CO_2 fixation by the haptophyte was stimulated by the addition of ammonium nitrate as well as Fe and Saharan dust. Intriguingly, the single-cell analysis using nanometer scale secondary ion mass spectrometry indicates that the increased CO_2 fixation by the haptophyte in treatments without added fixed N is likely an indirect result of the positive effect of Fe and/or P on UCYN-A N_2 fixation and the transfer of N_2-derived N to the haptophyte. Our results reveal a direct linkage between the marine carbon and nitrogen cycles that is fuelled by the atmospheric deposition of dust. The comparison of single-cell rates suggests a tight coupling of nitrogen and carbon transfer that stays balanced even under changing nutrient regimes. However, it appears that the transfer of carbon from the haptophyte to UCYN-A requires a transfer of nitrogen from UCYN-A. This tight coupling indicates an obligate symbiosis of this globally important diazotrophic association.
The ISME Journal (2015) 9, 1635–1647; doi:10.1038/ismej.2014.253; published online 23 December 2014

Introduction

Open ocean environments are generally characterized by the scarcity of nutrients, particularly bioavailable (fixed) nitrogen (N), that limits primary productivity (Karl *et al.,* 2002). In such oligotrophic environments, the activity of diazotrophs, prokaryotic microorganisms that mediate the fixation of atmospheric N_2 (Zehr *et al.,* 1998; LaRoche and Breitbarth, 2005), is favored as they can overcome N limitation as long as other nutrients are not limiting. Since the 1960s, the most studied diazotroph has been the nonheterocystous, filamentous cyanobacterium *Trichodesmium* spp. that contributes significantly to N_2 fixation in tropical and subtropical

oceans (Capone *et al.,* 2005). In addition, symbiotic relationships between diazotrophs and photosynthetic eukaryotes play a critical role in N_2 fixation and carbon (C) sequestration in the ocean (Carpenter and Foster, 2003, Karl *et al.,* 2012). Foster *et al.* (2011) investigated various marine diazotroph-diatom symbiotic associations and showed that substantial amounts of fixed N are transferred from the diazotroph to the host, resulting into enhanced diatom growth rates.

More recently, the importance of N_2-fixing unicellular cyanobacteria populations (UCYN-A, UCYN-B, UCYN-C) in the global N cycle has been recognized (Zehr *et al.,* 2001; Montoya *et al.,* 2004). Surveys based on quantitative PCR (qPCR) assays that target diazotroph abundance using the N_2 fixation marker gene *nifH* (which encodes the monomer of the Fe-subunit protein of the nitrogenase, the key enzyme for N_2 fixation) have revealed widespread distribution of the UCYN groups throughout the oceans (Church *et al.,* 2005a; Langlois *et al.,* 2008). The *nifH* gene phylotype abundances of UCYN-A (*Candidatus* Atelocyanobacterium thalassa; Thompson *et al.,* 2012) can dominate diazotrophic communities (Luo *et al.,* 2012) and can be found in more diverse environments than other diazotrophs (Short and Zehr, 2007;

Correspondence: A Krupke, Department of Marine Chemistry and Geochemistry, Woods Hole Oceanographic Institution, 360 Woods Hole Road, Fye 107C, Woods Hole, MA 02543, USA.
E-mail: akrupke@whoi.edu
[3]Current address: Department of Marine Chemistry and Geochemistry, Woods Hole Oceanographic Institution, Woods Hole, MA, USA.
[4]Current address: Max Planck Institute for Marine Microbiology, Bremen, Germany.
[5]Current address: Dalhousie University, Halifax, Nova Scotia, Canada.

![npg]
Nutrient effects on UCYN–A–haptophyte symbiosis
A Krupke *et al*

Rees *et al.,* 2009; Moisander *et al.,* 2010). Recently, UCYN-A has been found living in association with unicellular photosynthetic eukaryotes belonging to the *Haptophyta*, and more specifically, a prymnesiophyte (Thompson *et al.,* 2012; Hagino *et al.,* 2013; Krupke *et al.,* 2013, 2014). It has been hypothesized that the eukaryotic photosynthetic partner provides C compounds for UCYN-A and, in return, obtains N compounds from UCYN-A (Thompson *et al.,* 2012). Such an association seems mutually beneficial as the eukaryote cannot use N_2 as an N source and, from what is known so far, UCYN-A lacks the capability to use CO_2 as their C source (Zehr *et al.,* 2008; Tripp *et al.,* 2010; Thompson *et al.,* 2014).

Unfortunately, cultures of UCYN-A do not exist, and field experiments are necessary to understand nutrient requirements and environmental parameters that regulate the physiological interactions between UCYN-A and their eukaryotic partner. For *Trichodesmium* and complex marine microbial communities, it has been shown that diazotrophic activity can be limited by phosphorus (P) or iron (Fe), or be co-limited by both (Sañudo-Wilhelmy *et al.,* 2001; Mills *et al.,* 2004; Shi *et al.,* 2007), whereas eukaryotic phytoplankton are most often N limited. Currently, little is known about how UCYN-A responds to nutrient limitation. A recent study investigating the response of *nifH* expression of different diazotrophs to nutrient additions indicated that UCYN-A might be P limited in the tropical North Atlantic (Turk-Kubo *et al.,* 2012). To date, there are no reports on the effect of nutrient limitation on the photosynthetic partner of UCYN-A and/or this symbiosis.

Here, we conducted a wide range of nutrient amendment experiments near the Cape Verdean Islands to investigate the effect of nutrient additions on cellular CO_2 and N_2 fixation rates within the UCYN-A-haptophyte symbiosis. double catalyzed reporter deposition–fluorescence *in situ* hybridization (CARD–FISH) assays targeting UCYN-A cells, as well as their eukaryotic partner cells, allowed us to visualize the metabolic activity of UCYN-A at the single cell level using nanometer scale secondary ion mass spectrometry (nanoSIMS). In addition, we measured bulk N_2 fixation activity and used qPCR to assess UCYN-A *nifH* gene and *nifH* transcript abundances. The results of this study will help to understand the physiology of this globally important diazotrophic symbiosis and how it might be influenced by changes in the environment.

Materials and methods

Incubation experiments
Surface sea water (5–10 m depth) was collected at night using trace metal clean techniques and a diaphragm pump near the Cape Verdean Islands (16.79° N, 25.10° W) on board the R/V *Islandia* in May 2009. Sea water was transferred into acid-cleaned 4.5 l polycarbonate bottles and kept dark until further processing at the on-shore laboratory within 2–8 h of sampling. Incubation bottles were amended with nutrients, filled headspace free and closed with septa caps. Nutrient amendments resulted in 10 different treatments: (1) Ctr = control, no nutrients added, (2) N = NH_4NO_3 (ammonium nitrate), (3) Fe = $FeCl_3$ (ferric chloride), (4) P = NaH_2PO_4 (monosodium phosphate), (5) NP = $NH_4NO_3 + NaH_2PO_4$, (6) NFe = $NH_4NO_3 + FeCl_3$, (7) PFe = $NaH_2PO_4 + FeCl_3$, (8) NPFe = $NH_4NO_3 + NaH_2PO_4 + FeCl_3$, (9) DI = Saharan dust I and (10) DII = Saharan dust II (that is, 2 × Saharan dust DI). Final concentrations were: N (2 μM N), Fe (2 nM), P (0.2 μM), DI (2 mg l^{-1}) and DII (4 mg l^{-1}). The Saharan dust utilized in this study is the same as in Heller and Croot (2011), where the dust has been characterized in detail (that is, trace metal composition). Each treatment was prepared in quadruplicate.

All incubation bottles were placed in an incubator with continuously flowing surface sea water (± 3 °C *in situ* temperature) and shaded to 25% surface irradiance (blue lagoon, 172 Lee Filters, Seattle, WA, USA). After 24 h of incubation, three bottles were amended with 2.2 ml $^{15}N_2$ per l (98% + $^{15}N_2$, Sigma-Aldrich, St Louis, MO, USA) and 240 μM ^{13}C bicarbonate solution (H$^{13}CO_3^-$) (98% + $^{13}CO_2$, Silantes, Munich, Germany) using gas-tight syringes. The fourth bottle was amended with unlabeled bicarbonate solution and air to determine background natural abundance of ^{13}C and ^{15}N. All bottles were incubated for a second 24-h period.

Isotope ratio mass spectrometry
Experiments were stopped by filtering 2–3 l of sea water from the incubations onto pre-combusted (450 °C, 6 h) 25 mm GF/F filters (Whatman, St Louis, MO, USA). Filters were acidified with fuming HCl in a desiccator overnight, oven dried for 1 h at 55 °C and pelletized in tin cups. Particulate organic C and N and the relative abundances of ^{13}C and ^{15}N were determined through continuous flow isotope ratio mass spectrometry coupled to an elemental analyzer. Bulk N_2 fixation rates were then calculated following Montoya *et al.* (1996).

Nucleic acid extraction
Subsamples for DNA and RNA (1.5–2 l) were taken from each bottle that was amended with ^{13}C bicarbonate and $^{15}N_2$ gas (that is, triplicate samples) and filtered onto 47 mm Durapore (0.2 μM pore size; Millipore, Darmstadt, Germany) filters and stored at − 80 °C. Nucleic acids were extracted with the Qiagen (Hilden, Germany) DNA/RNA Plant Mini kit. Samples were prepared for extraction following Langlois *et al.* (2012). To facilitate cell lysis, 200 μl of lysozyme solution (5 mg ml^{-1} in TE buffer) was added initially into vials, vortexed, incubated at room temperature for 5 min and then the manufacturer's protocol was followed. DNA was eluted in 2 × 30 μl of TE buffer; RNA was eluted in 1 × 50 μl of

DEPC-treated water. DNA and RNA were stored at −80 °C until further analysis.

Reverse transcription–qPCR (RT–qPCR)
Eluted RNA was treated with Ambion's (Waltham, MA, USA) Turbo DNA-free kit to remove residual genomic DNA and reverse transcribed (RT) using the Super-Script III cDNA synthesis kit (Invitrogen, Karlsruhe, Germany) and the general *nifH2* (Zehr and McReynolds, 1989) and *nifH3* primers (Zani *et al.,* 2000). No RT controls were later used from randomly selected samples to confirm the absence of genomic DNA in RT–qPCR.

Quantitative PCR (qPCR and RT–qPCR) and Taq-Man Technology (St Louis, MO, USA) (including primer and probe sequences) were used according to Langlois *et al.* (2008) to determine the *nifH* abundance and the *nifH* gene expression levels of UCYN-A using the extracted DNA and the synthesized cDNA, respectively.

Double CARD–FISH assay
Aliquots (20 ml) of each incubation bottle were preserved in 1% paraformaldehyde for 24 h at 4 °C. Aliquots were filtered onto gold/palladium pre-sputtered 25 mm polycarbonate GTTP filters (0.2 μM pore size; Millipore), washed with 0.2 μM filtered sea water and stored at −20 °C.

Phylogenetic identification was performed through two separate rounds of CARD–FISH. First, we used the 18S rRNA oligonucleotide probe PRYM02 (5′-GGAATACGAGTGCCCCTGAC-3′) in combination with Alexa594 tyramides (Molecular Probes, Leiden, The Netherlands) targeting *Haptophyta* (Simon *et al.,* 2000) and following standard protocols (Pernthaler and Amann, 2004; Pernthaler *et al.,* 2004). After completing the first round of CARD–FISH, filter sections were washed in 1 × phosphate-buffered saline for 10–20 min in the dark and placed in 3% H_2O_2 solution for 20 min at room temperature in order to inactivate the inserted horseradish peroxidase and to prepare filter sections for the second CARD–FISH. Here, the oligonucleotide probe UCYN-A732 (5′-GTTACGGTCCAGTAG CAC-3′), which targeted the 16S rRNA specific for UCYN-A cells, and its corresponding helper probes Helper A-732 and Helper B-732 (5′-GCCTTCGCCAC CGATGTTCTT-3′ and 5′-AGCTTTCGTCCCTGAGTG TCA-3′) were applied to increase the probes' access to 16S rRNA target regions according to Krupke *et al.* (2013). During the second CARD–FISH application, fluorine (^{19}F)-labeled tyramides were used (that is, Oregon Green 488, Molecular Probes). Lastly, the cells were counterstained with 1 μg ml^{-1} DAPI (4',6-diamidino-2-phenylindol) for 10 min at room temperature in the dark.

The horseradish peroxidase-labeled oligonucleotide probes were used at working solutions of 8.42 pmol μl^{-1}, following dilution of stock solutions in the hybridization buffer (1:300; v-v).

All hybridizations were performed at optimal formamide concentrations to ensure maximal stringency (Krupke *et al.,* 2013); the oligonucleotides EUB338 (Amann *et al.,* 1990) or EUK516 (Amann *et al.,* 1990) were used as positive controls and the oligonucleotide NON338 (Wallner *et al.,* 1993) was used as a negative control.

Marking, microscopy and mapping for nanoSIMS
Laser markings were made near positively hybridized UCYN-A–haptophyte cells via a Laser Microdissection Microscope 6500 (Leica, Solms, Germany). Optical filter sets suitable for the applied tyramides during the CARD–FISH assays were used. Filter pieces were examined and microscopic pictures taken using a Zeiss Axioskop II fluorescence microscope (Zeiss, Oberkochen, Germany). Pictures were used for orientation during subsequent nanoSIMS analysis. Filter pieces were washed and air-dried before nanoSIMS analysis.

NanoSIMS measurements
Single-cell isotope ratios were measured and visualized using a Cameca NanoSIMS 50L instrument (Cameca, Gennevilliers, France). Before analysis, the area was pre-sputtered for 1–2 min with a defocused positively charged Cesium (Cs^+) primary ion beam to implant Cs^+ on the sample surface and get a sputter equilibrium. Then, sample surfaces were rastered with a 16 keV Cs^+ beam and a current between 1 and 3 pA. Primary ions were focused into a nominal ∼100 nm spot diameter. The primary ion beam was used to raster the analyzed area with an image size of 256 × 256 pixels and a dwelling time of 1 or 3 ms per pixel. Raster areas were usually 10 × 10 μM. Negatively charged secondary ions of carbon (C), fluorine (F), nitrogen (as CN) and sulfur (S) (that is, $^{12}C^-$, $^{13}C^-$, $^{19}F^-$, $^{12}C^{14}N^-$, $^{12}C^{15}N^-$ and $^{32}S^-$) were measured simultaneously in raster imaging mode by electron multiplier detectors.

All scans (40–50 planes) were corrected for drift of the beam and sample stage after acquisition. Isotope ratio images were created as the ratio of a sum of total counts for each pixel over all recorded planes with respect to the investigated isotope. Regions of interest around cell structures were circled and calculated using the automated threshold feature based on the look@nanosims software (Polerecky *et al.,* 2012). Cell dimensions were determined based on regions of interest.

Calculations
CO_2 and N_2 fixation rates (including C and N transfer rates) for individual cells were calculated using the equations listed below. The biovolume (V) was calculated from individual cell diameters and assuming a spherical shape for both UCYN-A and the haptophyte that had been confirmed

microscopically. The C content per individual UCYN-A cell was determined according to Verity *et al.* (1992):

$$Log[C] = -0.363 + (0.863 \times (Log(V))) \quad (1)$$

Estimates of C content per individual haptophyte cell were according to Strathmann (1967):

$$Log[C] = -0.422 + (0.758 \times (Log(V))) \quad (2)$$

The C content per cell (C_{con}) was converted into N content per cell (N_{con}) based on conversion factors provided by Tuit *et al.* (2004) assuming a modified Redfield ratio (C/N) of 8.6. The isotopic ratios ($R_C = {}^{13}C/{}^{12}C$ and $R_N = {}^{15}N/{}^{14}N$) based on region of interest selections and nanoSIMS analysis were used to calculate atom percent (AT%) enrichment of ${}^{13}C$ or ${}^{15}N$ by:

$$A_C = R_C/(R_C + 1) \quad (3)$$

$$A_N = R_N/(R_N + 1) \quad (4)$$

where A_C represents AT% enrichment of ${}^{13}C$ and A_N represents the AT% enrichment of ${}^{15}N$. The cell-specific C and N fixation (F_C or F_N) were calculated according to the length of incubation time after stable isotope amendments (that is, 24 h) with:

$$F_C = ({}^{13}C_{ex}/C_{SR}) \times C_{con} \quad (5)$$

$$F_N = ({}^{15}N_{ex}/N_{SR}) \times N_{con} \quad (6)$$

where ${}^{13}C_{ex}$ and ${}^{15}N_{ex}$ represent the AT% enrichment of ${}^{13}C$ and ${}^{15}N$ of the individual regions of interest corrected for the mean AT% ${}^{13}C$ and AT% ${}^{15}N$ at time 0, that is, ${}^{13}C$ and ${}^{15}N$ excess. The AT% enrichment of ${}^{13}C$ and ${}^{15}N$ at time 0 were determined on bulk samples using elemental analyzer–isotope ratio mass spectrometry. The elemental analyzer–isotope ratio mass spectrometry was calibrated for nonenriched and enriched samples with high instrument accuracy and precision (for example, 0.3651 ± 0.0000 ${}^{15}N$ atom % and 1.0658 ± 0.0004 ${}^{13}C$ atom % based on the mean and s.d. of caffeine standards. The AT% labeling of C (C_{SR}) and N (N_{SR}) substrates in the experimental bottle, that is, CO_2 and N_2, was calculated and corrected for the natural abundance of ${}^{13}C$ and ${}^{15}N$. This study presents measured AT% ${}^{13}C$ and AT% ${}^{15}N$ enrichment values of individual cells and utilizes these data to calculate single-cell CO_2 and N_2 fixation rates.

Statistical evaluations
Bulk N_2 fixation rates, *nifH* gene and *nifH* transcript abundances, and single-cell CO_2 and N_2 fixation results (including AT% ${}^{13}C$ and ${}^{15}N$ enrichment values) were statistically evaluated using SigmaStat 3.5 software (Systat Software Inc., San Jose, CA, USA). The equal variance within each treatment was first tested to proceed with a regular *t*-test for comparison between the control and each individual treatment (significance at $P < 0.05$). In instances

where a nonnormal distribution was detected, we applied the Mann–Whitney rank-sum test.

Results

Bulk N_2 fixation rates and nifH gene and nifH transcript abundance of UCYN-A
Bulk N_2 fixation activity across all nutrient treatments varied between 0.8 ± 0.1 and 1.3 ± 0.6 nmol l^{-1} N per day and did not differ significantly from the control (1.0 ± 0.2 nmol l^{-1} N per day; $P > 0.05$; Figure 1a). The *nifH* phylotype UCYN-A was detected by qPCR in all nutrient treatment incubation experiments at moderate abundances (10^3–10^4 *nifH* gene copies per l; Figure 1b), but no significant differences between any two treatments were observed ($P > 0.05$). The UCYN-A *nifH* transcript abundances were approximately one order of magnitude higher than *nifH* gene copies across all treatments (Figure 1b). The ratio of *nifH* transcript to *nifH* gene abundance is within the range previously reported for UCYN-A (Church *et al.,* 2005b; Turk-Kubo *et al.,* 2012). Overall, *nifH* transcript abundances did not differ significantly between any two treatments ($P > 0.05$).
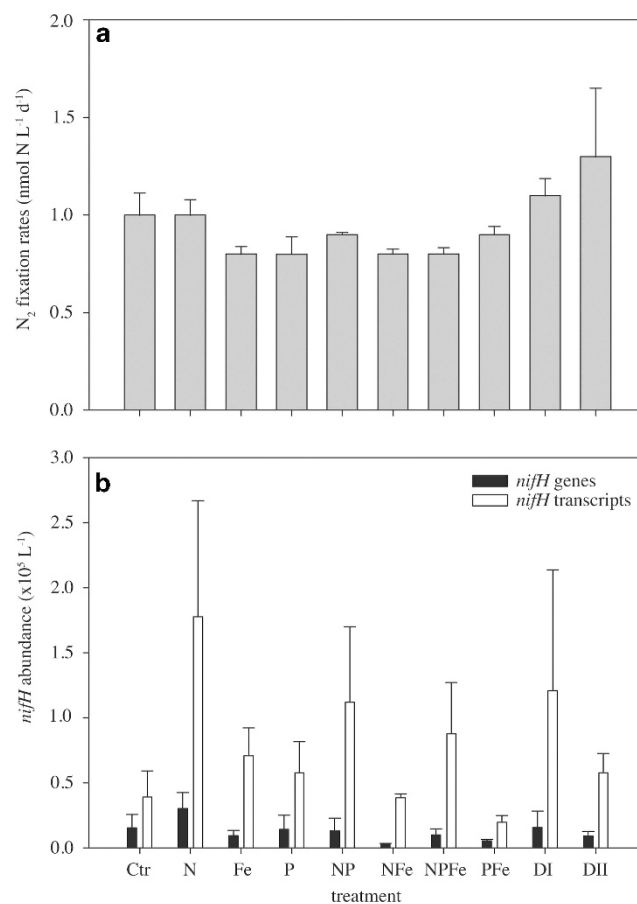

Figure 1 Mean bulk N_2 fixation rates (**a**), as well as mean UCYN-A *nifH* gene and *nifH* transcript abundance (**b**) with s.e. from incubation experiments across nutrient treatments as described in the Materials and Methods.

Visualization of UCYN-A–haptophyte associations
UCYN-A cells and partner haptophyte cells were simultaneously identified via the double CARD–FISH approach (Figures 2a, d and g, small inserts). The application of the UCYN-A-specific oligonucleotide probe (Krupke *et al.,* 2013) in concert with the deposition of halogenated (^{19}F) tyramides allowed us to verify the phylogenetic identification of UCYN-A cells and to image single-cell N_2 and CO_2 fixation within UCYN-A–haptophyte associations via nanoSIMS measurements (Figures 2a–i). Examples for individual associations in the control, N and Saharan dust DII treatments are shown in Figures 2a–i.

NanoSIMS measurements of all examined cells across all treatments gave average cell diameters and associated s.d. values of $0.83 \pm 0.15 \mu M$ for UCYN-A ($n = 44$ cells) and $1.66 \pm 0.23 \mu M$ for haptophyte cells ($n = 44$ cells). Biovolumes were calculated based on individual cell diameter following the termination of each treatment (Figures 3a and b and Supplementary Figures 1A–D). Overall, average biovolumes and associated s.d. values of UCYN-A cells across treatments ($0.33 \pm 0.17 \mu m^3$; $n = 36$) were not significantly different from the unamended control ($0.27 \pm 0.08 \mu m^3$; $n = 8$; $P > 0.05$).

In contrast to the UCYN-A, nutrient additions led to increased biovolumes of haptophyte cells. Except

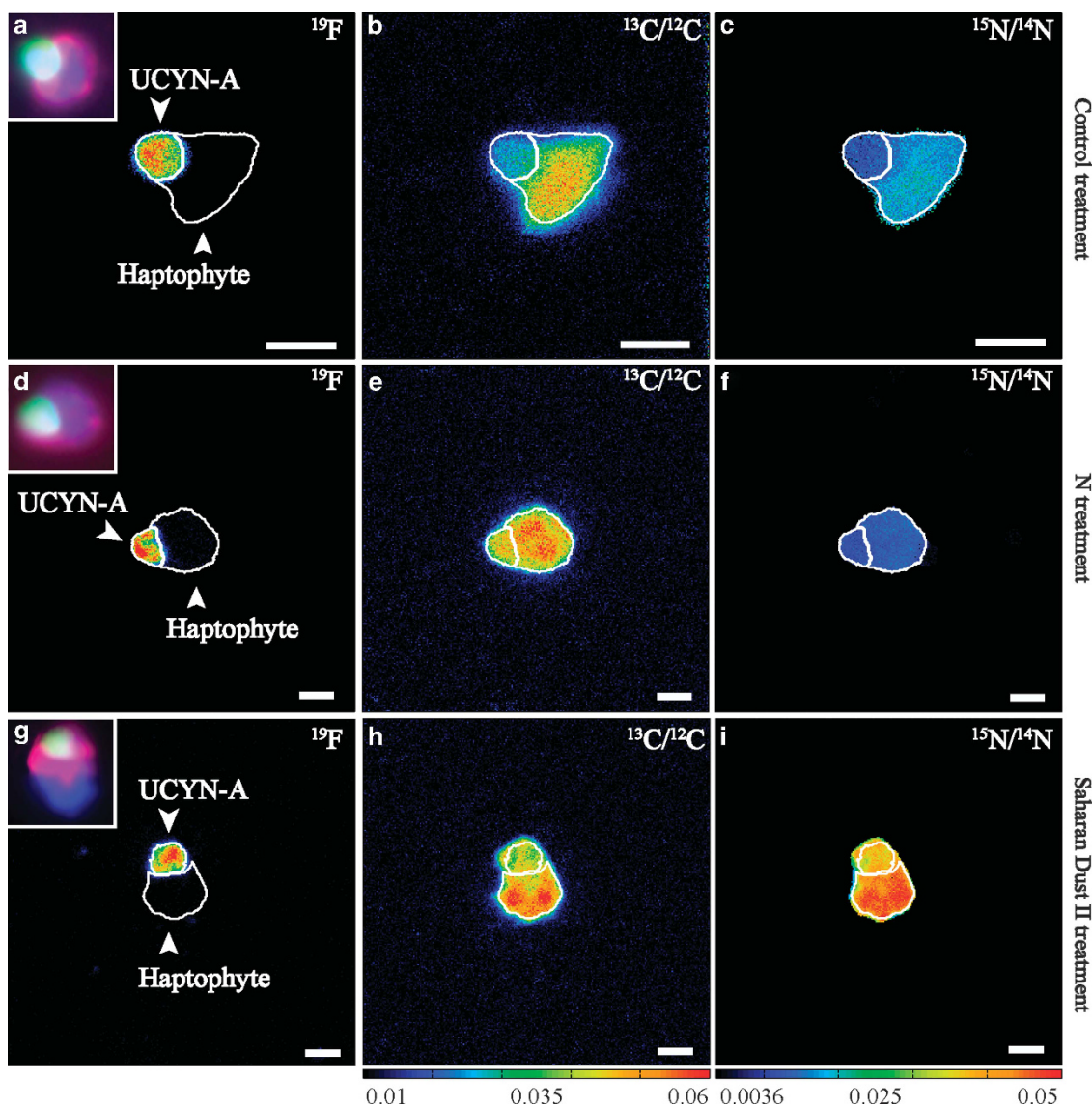**Figure 2** Visualization of the UCYN-A–haptophyte association according to the probe-conferred ^{19}F signal (left panels **a**, **d**, **g**) and single-cell activities based on isotope ratios of C ($^{13}C/^{12}C$ = middle panels **b**, **e**, **h**) and N ($^{15}N/^{14}N$ = right panels **c**, **f**, **i**) within different nutrient amendment incubation experiments. Inset panels on the left side show the corresponding epifluorescence images of the UCYN-A cells (green signal) and its associated haptophyte cell (red signal), as well as DAPI staining (blue signal) based on double CARD–FISH approach taken before nanoSIMS analysis. NanoSIMS images refer to different nutrient amendment incubation experiments: (**a–c**) Control = no nutrient added, (**d–f**) N = NH_4NO_3 addition, (**g–i**) DII = $4 \, mg \, l^{-1}$ Saharan dust. Warmer colors represent higher abundance of the heavier isotopes.
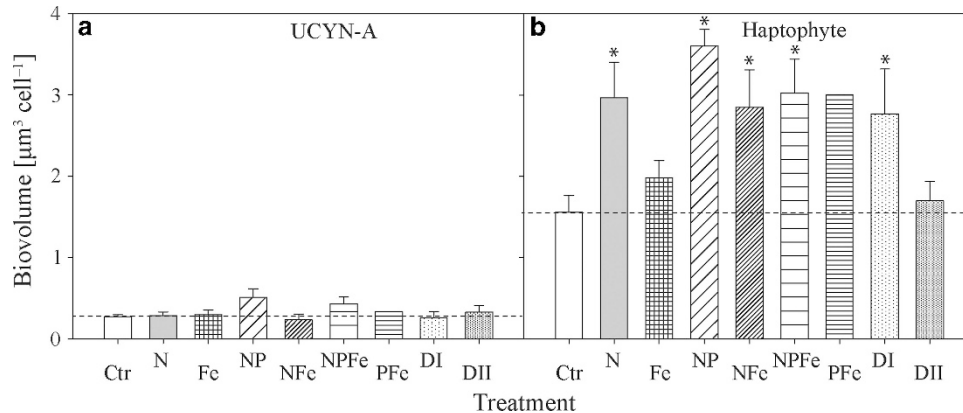
Figure 3 Mean biovolumes with s.e. for (**a**) UCYN-A and (**b**) the associated haptophyte cells in the different treatments as described in the Materials and Methods. The asterisks indicate a statistically significant difference compared with the control. No statistics were performed on results from the PFe treatment because only one UCYN-A–haptophyte association was found. Dashed lines indicate mean values of control measurements.

for the Fe and Saharan dust DII treatments, calculated biovolumes in the nutrient treatments were significantly larger ($3.05 \pm 0.16 \, \mu m^3$; $n = 27$) than the control ($1.56 \pm 0.21 \, \mu m^3$; $n = 8$; $P < 0.05$; Figure 3b). The largest biovolume was observed in the NP treatment ($3.60 \pm 0.20 \, \mu m^3$). Generally, estimated biovolumes for associated haptophyte cells were ∼3–10 times larger than values for UCYN-A cells (Figures 3a and b).

Inorganic carbon fixation in haptophyte cells and transfer to UCYN-A cells
All investigated cells were enriched in ^{13}C, indicating inorganic C fixation by these symbioses (Figures 4a–d and Supplementary Figures 2A and B). The actual CO_2 fixation might be even higher; a recent study by Musat *et al.* (2014) revealed that the application of FISH and CARD–FISH techniques before nanoSIMS measurements can lower cellular ^{13}C and ^{15}N enrichments, leading to the underestimation of rates. As UCYN-A does not have any genes for CO_2 fixation, we regard any ^{13}C enrichment as originating from CO_2-derived C transfer from the host.

The ^{13}C enrichments of haptophyte cells were not significantly different between treatments ($P > 0.05$; Figure 4c and Supplementary Table 1). In comparison, the ^{13}C enrichment in UCYN-A cells was significantly elevated in the following treatments: (1) Fe, (2) NP, (3) NPFe and (4) Saharan dust DII ($P < 0.05$; Table 1 and Figure 4a). Across treatments, ^{13}C enrichments in haptophyte cells were up to twice as high as the ^{13}C enrichment of their respective UCYN-A symbiont (Figures 4a and c and Supplementary Figures 3A–I).

Estimated CO_2 fixation rates in haptophyte cells increased significantly in all nutrient treatments compared with the control ($P < 0.05$), except in the Saharan dust DII treatment (Table 1 and Figure 4d). CO_2 fixation rates by haptophytes were up to seven times greater than the transfer rates of the fixed C to

UCYN-A (Table 1 and Figures 4b and d). The calculated CO_2-derived C transfer rates among UCYN-A cells were up to 3 times higher after nutrient addition than in the control treatment and differed significantly from the control in the Fe, NP and the NPFe treatments ($P < 0.05$; Table 1 and Figure 4b). Elevated CO_2-derived C transfer to UCYN-A was also observed in the PFe treatment, but the available data set for this treatment is limited because only one symbiosis could be found. No data are available from the P-only treatment because no double-hybridized UCYN-A–haptophyte associations were found in the investigated sample. Overall, a strong correlation in the ^{13}C enrichment ($r = 0.79$) as well as in the CO_2 fixation rates ($r = 0.60$) between UCYN-A and haptophyte cells were detected across all treatments (Figures 5a and b).

Nitrogen fixation in UCYN-A and transfer of nitrogen to associated haptophyte cells
In contrast to UCYN-A, which lacks the ability to fix CO_2 but can fix N_2, the haptophyte cannot perform N_2 fixation; thus, we regard any ^{15}N enrichment in the haptophyte as N_2-derived N transfer from UCYN-A. Within each treatment, the ^{15}N enrichment between individual UCYN-A cells and their respective haptophyte host showed similar patterns (Figures 4e and g and Supplementary Figures 3A–I). Nonetheless, the ^{15}N enrichment and N_2-derived N transfer rates among individual haptophyte cells, as well as individual UCYN-A cells, differed significantly between treatments (Figures 4e–h). In particular, UCYN-A cells were significantly enriched in ^{15}N (2–3-fold) in the iron and Saharan dust (Fe, DI, DII) additions compared with the control ($P < 0.05$; Figure 4e). This resulted in corresponding N_2 fixation rates for UCYN-A cells that were significantly higher in the Fe, Saharan dust DI and DII treatments than in the control ($P < 0.05$; Table 1 and Figure 4f). N_2 fixation rates were not significantly different from the control when inorganic N (that is,
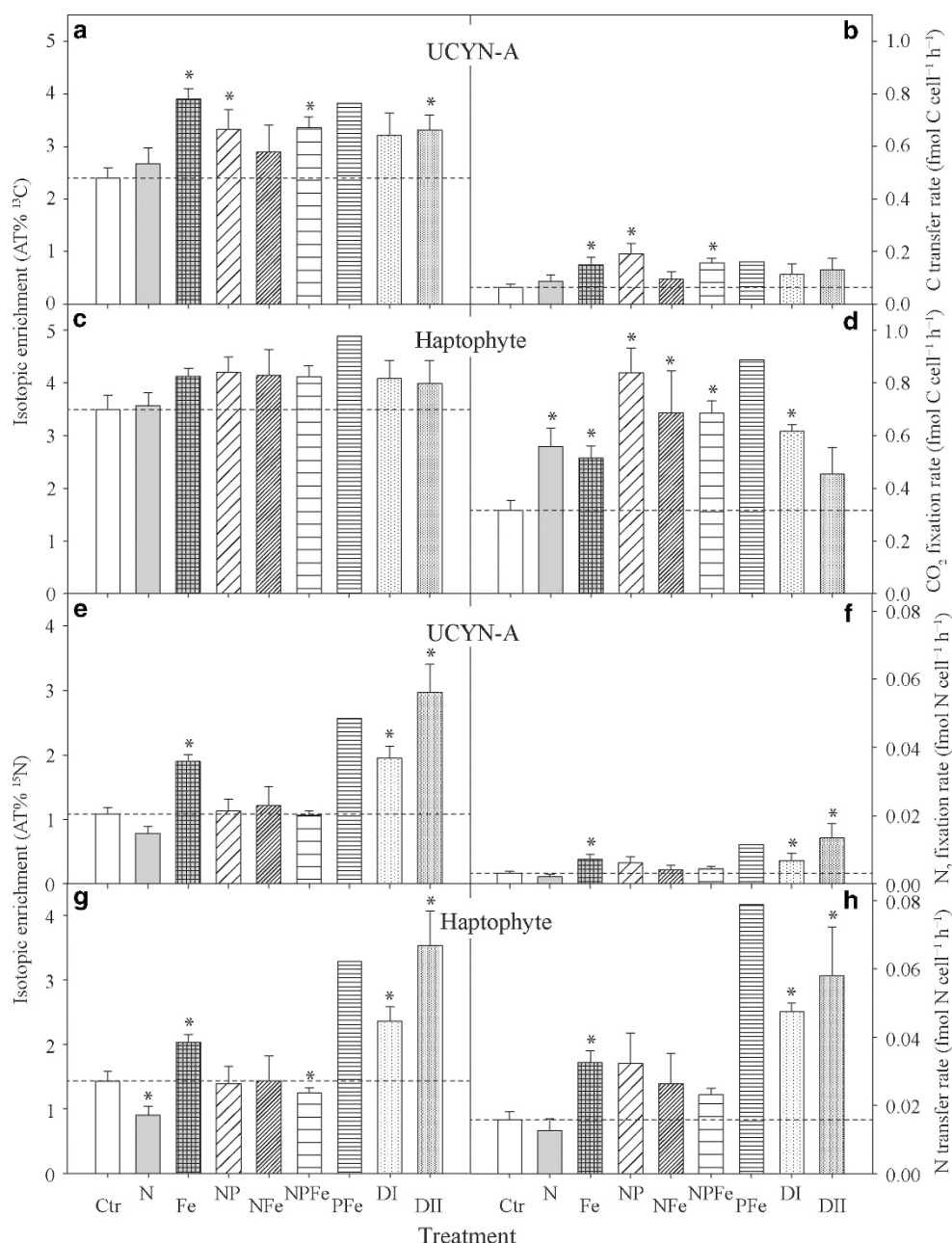
Figure 4 NanoSIMS measurements for the association between UCYN-A and their associated haptophytes from the nutrient amendment experiments. The panels on the left side represent the isotope enrichment in AT% for individual cells for ^{13}C (**a**, UCYN-A; **c**, haptophyte) and ^{15}N (**e**, UCYN-A; **g**, haptophyte). The panels on the right side (**b**, **d**, **f**, **h**) show the corresponding single-cell activity in fmol cell^{-1} h^{-1} for CO_2 and N_2 fixation, as well as C and N transfer rates for individual UCYN-A and partner haptophyte cells, calculated based on obtained nanoSIMS values (AT%) and cell dimension analysis. Treatments are as described in Materials and Methods. The asterisk symbol indicates means that are significantly different from the control at a $P < 0.05$ significance level. No statistics were performed on the PFe treatment. Dashed lines indicate mean values of control measurements.

NH_4NO_3) was available (Table 1 and Figure 4f), that is, N_2 fixation was not inhibited by the presence of fixed N.

The ^{15}N enrichment in haptophyte cells was significantly enhanced (2–3-fold) following Fe and Saharan dust DI and DII additions ($P < 0.05$; Figure 4g). The PFe treatment also yielded elevated ^{15}N that was nearly twice as high as the control values (Figure 4g and Supplementary Table 1).

In comparison, ^{15}N enrichment within haptophyte cells dropped significantly in the N treatment, as well as in the NPFe treatment ($P < 0.05$; Figure 4g and Supplementary Table 1). Corresponding N_2-derived N transfer rates to haptophyte cells increased in all nutrient additions compared with the control experiment, except in treatments in which fixed N was added, where rates were not significantly different from the control (Table 1 and

Figure 4h). The N_2-derived N transfer rates to haptophyte cells were significantly enhanced in the Fe, Saharan dust DI and DII treatments relative to the control ($P<0.05$; Table 1 and Figure 4h). A high rate of 0.08 fmol N cell^{-1} h^{-1} was also observed in the single haptophyte cell from the PFe treatment

(about five times the rate of the control; Table 1 and Figure 4h). Overall, strong correlations in the ^{15}N enrichment ($r=0.98$) as well as in N_2 fixation rates or transfer rates ($r=0.81$) between UCYN-A and haptophyte cells were detected across all treatments (Figures 5c and d).

Table 1 Summary of nanoSIMS analysis for the UCYN-A–haptophyte association from nutrient incubation experiments conducted on surface seawater samples collected from Cape Verde in May 2009

Experiment (treatment)	N^a	CO_2 fixation or C transfer rate (fmol C cell^{-1} h^{-1}) Mean ± s.d.		N_2 fixation or N transfer rate (fmol N cell^{-1} h^{-1}) Mean ± s.d.	
		UCYN-A	*Haptophyte*	*UCYN-A*	*Haptophyte*
Ctr	8	0.06 ± 0.01	0.32 ± 0.04[b]	0.0031 ± 0.0005	0.0158 ± 0.0024
N	8	0.09 ± 0.02	0.56 ± 0.07[b]	0.0020 ± 0.0007	0.0127 ± 0.0034
Fe	5	0.15 ± 0.03[b]	0.51 ± 0.05[b]	0.0072 ± 0.0014[b]	0.0326 ± 0.0034[b]
NP	5	0.19 ± 0.04[b]	0.84 ± 0.09[b]	0.0062 ± 0.0017	0.0323 ± 0.0089
NFe	4	0.09 ± 0.03	0.69 ± 0.16[b]	0.0041 ± 0.0014	0.0264 ± 0.0088
NPFe	5	0.16 ± 0.02[b]	0.68 ± 0.05[b]	0.0044 ± 0.0008	0.0231 ± 0.0018
Pfe	1	0.16[c]	0.89[c]	0.0115[c]	0.0789[c]
DI	4	0.11 ± 0.04	0.62 ± 0.02[b]	0.0069 ± 0.0021[b]	0.0475 ± 0.0023[b]
DII	4	0.13 ± 0.04	0.45 ± 0.10	0.0134 ± 0.0042[b]	0.0580 ± 0.0144[b]

Abbreviations: Ctr, controls; nanoSIMS, nanometer scale secondary ion mass spectrometry.
The mean and s.d. are listed for CO_2 and N_2 fixation and transfer rates for individual UCYN-A and partner haptophyte cells.
[a]Number of cells measured in each treatment.
[b]Significantly different from control measurements.
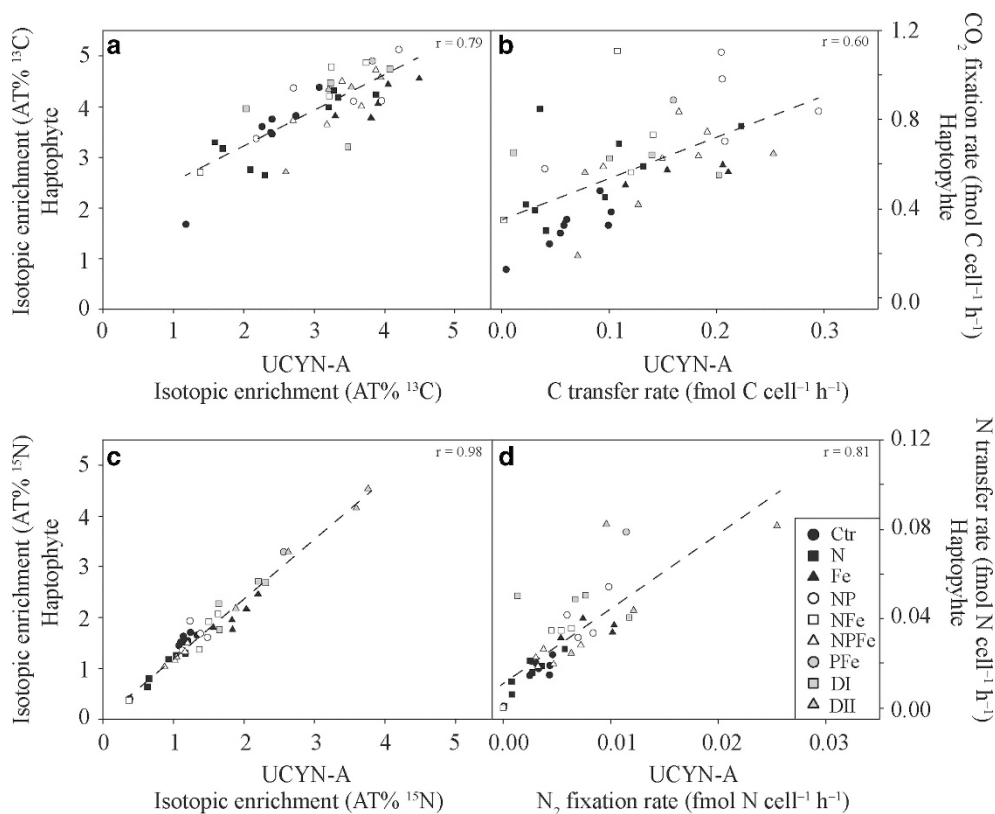[c]Based on one UCYN-A–haptophyte symbiosis.

Figure 5 Single-cell enrichments and rates for (**a**, **b**) carbon in AT% ^{13}C and fmol C cell^{-1} h^{-1}, respectively, and for (**c**, **d**) nitrogen in AT% ^{15}N and fmol N cell^{-1} h^{-1}, respectively, within individual associations between UCYN-A and its corresponding haptophyte partner cell across all treatments. Dashed lines represent regression lines and their corresponding *r*-values are depicted within each panel. Treatments are as described in Materials and Methods.

Unknown structures within the UCYN-A–haptophyte association

In incubations with NH_4NO_3, a third structure was observed in some UCYN-A–haptophyte associations ($n = 6$) (Figures 6a–f). Besides weak DAPI signals, these structures were found because of their distinct C isotopic signature revealed by nanoSIMS measurements. This enigmatic structure was slightly smaller than UCYN-A cells, with a diameter and s.d. of $0.70 \pm 0.06\,\mu M$ ($n = 6$) and a volume of $0.21 \pm 0.06\,\mu m^3$ ($n = 6$). These structures were highly enriched in ^{13}C (AT% ^{13}C 5.16 ± 0.44), but lower in ^{15}N (AT% ^{15}N 0.54 ± 0.06) compared with both UCYN-A and the haptophyte. On average, these structures were approximately two-thirds more enriched in ^{13}C than UCYN-A cells and approximately one-third more than haptophyte cells. Furthermore, these structures were ~ 2.5 times less enriched in ^{15}N than UCYN-A cells and 3 times less enriched than haptophyte cells across all treatments.

Discussion

The N_2 fixation rates (bulk and single cell) reported here represent minimum fixation rates; the common $^{15}N_2$ gas tracer addition method ('bubble method') was applied to the incubation experiments that has been shown to underestimate N_2 fixation (Mohr *et al.,* 2010a; Großkopf *et al.,* 2012; Wilson *et al.,* 2012). Given that the stable isotope addition experiments were initiated at the same time with the same initial microbial community from a common seawater sample, and treated with the same conditions except for the nutrient addition treatments, it is reasonable to assume that the 'bubble method' affected N_2 fixation rates in all treatments in the same manner. Hence, the relative response of N_2 fixation to the nutrient additions is comparable between treatments.

The open surface waters in the vicinity of Cape Verde are chronically depleted in macronutrients, particularly fixed N species, and are therefore
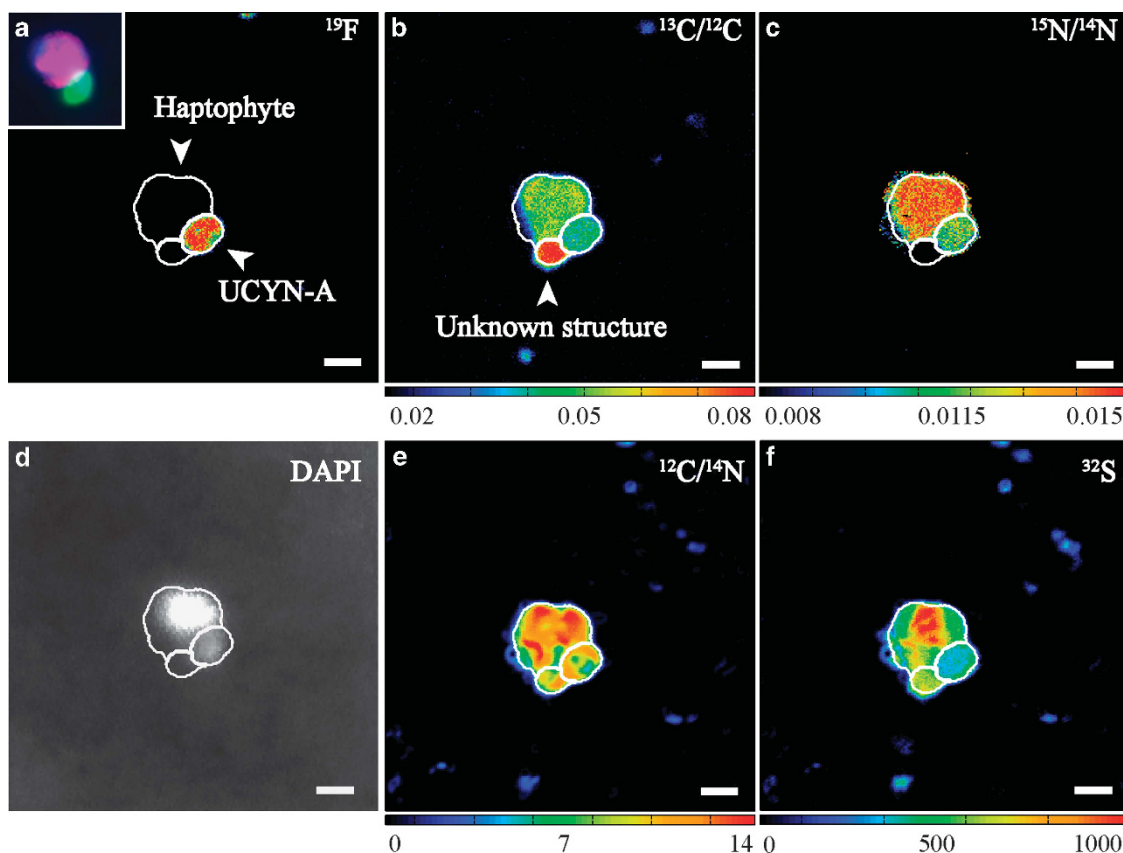

Figure 6 NanoSIMS measurements visualizing the 'unknown structure' found attached to a UCYN-A–haptophyte association within the NP treatment. (**a**) The probe-conferred ^{19}F signal and the corresponding epifluorescence images of the UCYN-A cells (green signal) and its associated haptophyte cell (red signal), as well as DAPI staining (blue signal) based on double CARD–FISH approach taken before nanoSIMS analysis (small inset panel). (**b**) Carbon enrichment as $^{13}C/^{12}C$, (**c**) nitrogen enrichment as $^{15}N/^{14}N$, (**d**) black and white image of the DAPI signals, (**e**) carbon and nitrogen distribution as $^{12}C/^{14}N$ * 1000 and (**f**) sulfur as ^{32}S. An unknown structure attached to the UCYN-A association was observed that is highly enriched in C, but lower in N and had a weak DAPI signal (**b**, **c**, **d**). In addition to carbon and nitrogen (**b**, **c**, **e**) the structure contained sulfur (**f**). Such a structure was only found when inorganic nitrogen was added. Warmer colors represent higher abundance of the heavier isotopes. Brighter white DAPI signals indicate stronger staining because of more DNA.

1644

thought to favor the abundance and activity of N_2-fixing microorganisms (Voss *et al.,* 2004). Bulk N_2 fixation rates were similar to rates previously reported from the subtropical North Atlantic (Mills *et al.,* 2004; LaRoche and Breitbarth, 2005), as well as other oligotrophic sites (Falcón *et al.,* 2004; Sohm *et al.,* 2011; Luo *et al.,* 2012). Across all nutrient treatments, bulk N_2 fixation rates were neither significantly stimulated nor suppressed, suggesting that N_2 fixation was neither limited by any of the added nutrients (or their combination) at this particular time nor inhibited in the presence of fixed N. However, it is also possible that the added nutrients affected bulk rates at timescales not considered here. As the bulk N_2 fixation rates in this study represent community-wide responses, these results say little about *nifH* phylotype-specific responses. Turk-Kubo *et al.* (2012) recently found that changes in N_2 fixation upon Fe and/or P addition were spatially heterogeneous in the tropical North Atlantic. They further reported that Fe and P additions caused varying responses among different phylotypes, suggesting that not all diazotrophs are limited by the same nutrient in time and space. For example, diazotrophs in the western tropical North Atlantic appeared to be Fe limited, whereas they were P limited in the eastern tropical North Atlantic. In particular, the uncultured cyanobacterial group A (UCYN-A; Thompson *et al.,* 2012) responded to additions of P with increased *nifH* gene expression, indicating P limitation of diazotrophs despite the lack of a measurable response in bulk N_2 fixation rates (Turk-Kubo *et al.,* 2012). Here, we determined UCYN-A gene expression patterns upon nutrient additions including N, Fe, P and Saharan dust. In contrast to Turk-Kubo *et al.* (2012), there were no significant responses in *nifH* gene expression to any of the added nutrients (alone or in combination). This might be partially because of the larger variation in the transcript abundance seen in this study. Although all RNA samples were taken within a 3-h time window, diel cycling of *nifH* gene expression could be responsible for this variation. For example, *nifH* transcript abundance can change by more than one order of magnitude within 3 h in *Crocosphaera watsonii* (Mohr *et al.,* 2010b). For UCYN-A, both diel (Church *et al.,* 2005b; Zehr *et al.,* 2008) and non-diel (Turk-Kubo *et al.,* 2012) expressions of *nifH* have been found, and these findings suggest that *nifH* expression in UCYN-A is not yet fully understood.

The UCYN-A have been found to live in association with a phototrophic eukaryote, more specifically a haptophyte (Thompson *et al.,* 2012; Hagino *et al.,* 2013; Krupke *et al.,* 2013, 2014). A symbiotic lifestyle originally had been suggested because of the reduced genome size and in particular the absence of several genes required for carbon fixation in UCYN-A (Zehr *et al.,* 2008; Tripp *et al.,* 2010). It was shown that the two partners in this symbiotic association, that is, the haptophyte and UCYN-A,

exchange C and N compounds; the haptophyte supplies CO_2-derived C and UCYN-A supplies N_2-derived N (Thompson *et al.,* 2012; Krupke *et al.,* 2013). This symbiotic association raises questions about its nutrient requirements and the interdependence of the two partner organisms, especially given that phytoplankton are usually affected by N limitation, whereas diazotrophs are considered limited by either P, Fe or both in the eastern tropical Atlantic. In order to address the question of nutrient limitation, we evaluated single-cell N_2 and CO_2 fixation activities by the UCYN-A–haptophyte association under different nutrient additions. The response of UCYN-A to the different nutrient treatments was unexpected given the fact that bulk N_2 fixation rates showed no clear response and that there were no significant changes in the *nifH* expression. We found that N_2 fixation by UCYN-A was clearly stimulated by the addition of Saharan dust. In addition, UCYN-A activity was also stimulated by the addition of Fe, suggesting that the Saharan dust served as a source of Fe. An increase in UCYN-A abundance in response to dust has been observed in a comparable experiment in the Atlantic, although the authors did not see a change in abundance in their Fe treatment (Langlois *et al.,* 2012). The deposition of dust in the marine environment may also release P in addition to Fe (Ridame and Guieu, 2002; Bonnet and Guieu, 2004). We could not determine the effect of P alone on the N_2 fixation rates by UCYN-A because of the lack of associations in that treatment, but our results from the PFe treatment indicated elevated N_2 fixation by UCYN-A relative to the control. However, these results have to be interpreted with caution because only one symbiosis was detected in that treatment. The combined results, however, suggest that UCYN-A were Fe limited with a possible Fe and P co-limitation, and that UCYN-A had the capability to utilize Saharan dust as a significant source of Fe and possibly other elements too.

The haptophyte partner responded to all nutrient additions with increased CO_2 fixation, including treatments that contained no added N. This finding contradicts classical observations of N limitation in phytoplankton; however, in all treatments without added fixed N, the haptophyte received significant amounts of N from their UCYN-A partner cell, indicating that N_2 fixation in UCYN-A and the subsequent transfer of N_2-derived N is an important source for the haptophyte. It further implies that the increase in CO_2 fixation by the haptophyte in treatments without added N is likely an indirect result of the positive effect of Fe and/or P on UCYN-A N_2 fixation and suggests that the haptophytes were N limited at the time of our study. In treatments where fixed N was added in combination with Fe or P (or both), the haptophyte could have either switched between the added N and the N_2-derived N from UCYN-A or used both sources simultaneously. Under typical oligotrophic conditions,

however, N_2 fixation by UCYN-A is likely to be the main source of fixed N for the haptophyte, fuelled by the atmospheric deposition of Fe through dust at this study site.

The strong correlation between the ^{15}N isotope enrichment in the haptophyte and the ^{15}N isotope enrichment in UCYN-A (and the similarly strong correlation between the ^{13}C isotope enrichments in both organisms) indicates a mutually beneficial relationship and a significant degree of dependence of both organisms on each other. On average, UCYN-A cells assimilated $16.4 \pm 7.1\%$ of all C fixed by the haptophyte and the haptophyte cells assimilated $85.4 \pm 5.1\%$ of N fixed by UCYN-A. These values are similar to recent findings that show UCYN-A transferring up to 95% of its fixed N to the host, and in turn receiving $\sim 17\%$ of the C fixed from the host (Thompson *et al.,* 2012). A similar transfer of C and N has also been reported for symbiotic relationships between diatoms and N_2-fixing cyanobacteria (diazotroph-diatom symbiotic associations) (Foster *et al.,* 2011). Similar to our study, other field studies have shown that fixed N is rapidly transferred (that is, $\leqslant 24$ h), for example, from heterocysts to vegetative cells in *Aphanizomenon* sp. populations (Ploug *et al.,* 2010), as well as within diazotroph-diatom symbiotic associations (Foster *et al.,* 2011). These results indicate an efficient nutrient transfer between the two partner cells. However, the exact mechanisms that allow for rapid nutrient exchange and the type of compounds that are exchanged remain unknown. Interestingly, the increase in CO_2 fixation triggered by fixed inorganic N addition alone did not result in an increased transfer of CO_2-derived C to UCYN-A or to an increased transfer of N_2-derived N from UCYN-A to the haptophyte. Combined, these results suggest that a simple increase in primary productivity (possibly triggered by an external source of fixed N) does not automatically result in elevated C transfer to the symbiont, but that any C transfer is coupled to transfer of N from UCYN-A to the haptophyte. The strong correlations of C and N enrichments between both organisms under changing nutrient regimes imply that the transfer of C and/or N between host and symbiont is concomitant and highly regulated. This tight coupling in C and N metabolism stays balanced even under changing nutrient regimes and indicates that the association between UCYN-A and the haptophyte is an 'obligate' symbiosis (Krupke *et al.,* 2014; Thompson *et al.,* 2014).

Interestingly, we did not observe an inhibition of UCYN-A *nifH* expression and N_2 fixation when fixed N was added as ammonium nitrate. However, other organisms in the incubations (for example, other phytoplankton) might have rapidly taken up the added fixed N, preventing an inhibition of *nifH* expression or resulting in temporary inhibition of *nifH* expression only. Thus, inhibitory effects in *nifH* gene expression may have been missed at the end of the incubation time. Other cultivated members of the UCYN groups have also been shown to be nonresponsive to additions of nitrate (Dekaezemacker and Bonnet, 2011; Großkopf and LaRoche, 2012), and as the understanding of the UCYN-A physiology is in its early stages, it is possible that N_2 fixation in UCYN-A is not inhibited in the presence of fixed N.

We observed an unknown structure within the UCYN-A–haptophyte association that occurred in treatments that had ammonium nitrate additions. Presently, it is unclear what this structure might represent: it could be a C-storage compartment, for example carbohydrates. This structure may also be an attached unidentified microorganism as it contains C, N and sulfur (S), and a weak DAPI signal was observed. Diffuse or very weak DAPI signals are common for small cells. Because this structure is more enriched in ^{13}C than the photosynthetic partner algae of UCYN-A, it may be an unidentified photosynthetic or chemolithoautotrophic organism. Symbiotic relationships between marine diatoms and multiple unicellular N_2-fixing cyanobacterial endosymbionts have been reported previously (Villareal, 1991; Carpenter and Janson, 2000). Here, photosynthetic activity can be restricted to the algal partner cell that supplies the other partners with fixed C compounds. Similar observations have been made in tripartite symbiotic relationships between fungi, algae and cyanobacteria (Honegger, 2001). Flexibility of the epibiont load (potential tripartite symbiosis) might offer competitive growth advantages for the haptophyte and/or UCYN-A under varying nutrient environments. The identification of a possible third partner cell will be an important step in understanding the complex interactions in this symbiosis.

Concluding remarks
This study provides the first insight into the physiological responses of field populations of the UCYN-A–haptophyte symbiosis to nutrient addition. Our results suggest that the presence of fixed N does not necessarily inhibit N_2 fixation and highlight that Fe (including Fe from Saharan dust deposition) and P inputs are major factors influencing N_2 fixation activity by UCYN-A. The subsequent transfer of fixed N to the photosynthetic partner haptophyte indirectly fuels primary productivity. The discovery of a third microstructure within the UCYN-A–haptophyte association, possibly an unknown cell, emphasizes the complexity of interactions among microorganisms in oligotrophic surface waters. Future efforts to gather genetic information on the metabolic repertoire of the associated haptophyte will help to unravel mechanisms and potential pathways regulating the C and N exchange within this association and may provide critical information for future isolation attempts of both partner cells. Here, we provide evidence for a tight coupling of C and N exchange within this

symbiosis in the Atlantic Ocean that may represent a different ecotype (Thompson *et al.,* 2014) than previously reported (Thompson *et al.,* 2012). The determined metabolic activities, cell diameters and biovolumes of the two partner cells will be helpful to deepen our understanding of their roles in the global C and N cycles.

Conflict of Interest

The authors declare no conflict of interest.

References

Amann RI, Binder BJ, Olson RJ, Chisholm SW, Devereux R, Stahl DA. (1990). Combination of 16S Rrna-targeted oligonucleotide probes with flow cytometry for analyzing mixed microbial populations. *Appl Environ Microbiol* **56**: 1919–1925.

Bonnet S, Guieu C. (2004). Dissolution of atmospheric iron in seawater. *Geophys Res Lett* **31**: 1–4.

Capone DG, Burns JA, Montoya JP, Subramaniam A, Mahaffey C, Gunderson T *et al.* (2005). Nitrogen fixation by *Trichodesmium* spp.: an important source of new nitrogen to the tropical and subtropical North Atlantic Ocean. *Glob Biogeochem Cycles* **19**: 1–17.

Carpenter EJ, Foster RA. (2003). Marine cyanobacterial symbioses. In: Rai AN, Bergman B, Rasmussen U (eds) *Cyanobacteria in Symbiosis.* Kluwer Academic Publishers: Dordrecht, the Netherlands, pp 11–17.

Carpenter EJ, Janson S. (2000). Intracellular cyanobacterial symbionts in the marine diatom *Climacodium frauenfeldianum* (Bacillariophyceae). *J Phycol* **36**: 540–544.

Church MJ, Jenkins BD, Karl DM, Zehr JP. (2005a). Vertical distributions of nitrogen-fixing phylotypes at stn ALOHA in the oligotrophic North Pacific Ocean. *Aquat Microb Ecol* **38**: 3–14.

Church MJ, Short CM, Jenkins BD, Karl DM, Zehr JP. (2005b). Temporal patterns of nitrogenase gene (*nifH*) expression in the oligotrophic North Pacific Ocean. *Appl Environ Microbiol* **71**: 5362–5370.

Dekaezemacker J, Bonnet S. (2011). Sensitivity of N_2 fixation to combined nitrogen forms (NO_3^- and NH_4^+) in two strains of the marine diazotroph *Crocosphaera watsonii* (Cyanobacteria). *Mar Ecol Prog Ser* **438**: 33–46.

Falcón LI, Carpenter EJ, Cipriano F, Bergman B, Capone DG. (2004). N_2 fixation by unicellular bacterioplankton from the Atlantic and Pacific Oceans: phylogeny and *in situ* rates. *Appl Environ Microbiol* **70**: 765–770.

Foster RA, Kuypers MMM, Vagner T, Paerl RW, Musat N, Zehr JP. (2011). Nitrogen fixation and transfer in open ocean diatom-cyanobacterial symbioses. *ISME J* **5**: 1484–1493.

Großkopf T, LaRoche J. (2012). Direct and indirect costs of dinitrogen fixation in *Crocosphaera watsonii* WH8501 and possible implications for the nitrogen cycle. *Front Aquat Microbiol* **3**: 1–10.

Großkopf T, Mohr W, Baustian T, Schunck H, Gill D, Kuypers MMM *et al.* (2012). Doubling of marine dinitrogen-fixation rates based on direct measurements. *Nature* **488**: 361–364.

Hagino K, Onuma R, Kawachi M, Horiguchi T. (2013). Discovery of an endosymbiotic nitrogen-fixing cyanobacterium UCYN-A in *Braarudosphaera bigelowii* (prymnesiophyceae). *PLoS One* **8**: e81749.

Heller M, Croot P. (2011). Superoxide decay as a probe for speciation changes during dust dissolution in Tropical Atlantic surface waters near Cape Verde. *Mar Chem* **126**: 37–55.

Honegger R. (2001). The symbiotic phenotype of lichen-forming ascomycetes. In Hock (ed), *Fungal Associations.* Springer-Verlag: Berlin, Heidelberg, pp 165–188.

Karl D, Michaels A, Bergman B, Capone D, Carpenter E, Letelier R *et al.* (2002). Dinitrogen fixation in the world's oceans. *Biogeochemistry* **57**: 47–98.

Karl DM, Church MJ, Dore JE, Letelier RM, Mahaffey C. (2012). Predictable and efficient carbon sequestration in the North Pacific Ocean supported by symbiotic nitrogen fixation. *Proc Natl Acad Sci USA* **109**: 1842–1849.

Krupke A, Lavik G, Halm H, Fuchs BM, Amann RI, Kuypers MM. (2014). Distribution of a consortium between unicellular algae and the N2 fixing cyanobacterium UCYN-A in the North Atlantic Ocean. *Environ Microbiol* **16**: 3153–3167.

Krupke A, Musat N, LaRoche J, Mohr W, Fuchs BM, Amann RI *et al.* (2013). In situ identification and N_2 and C fixation rates of uncultivated cyanobacteria populations. *Syst Appl Microbiol* **36**: 259–271.

Langlois R, Mills MM, Ridame C, Croot P, LaRoche J. (2012). Diazotrophic bacteria respond to Saharan dust additions. *Mar Ecol Prog Ser* **470**: 1–14.

Langlois RJ, Hummer D, LaRoche J. (2008). Abundances and distributions of the dominant *nifH* phylotypes in the Northern Atlantic Ocean. *Appl Environ Microbiol* **74**: 1922–1931.

LaRoche J, Breitbarth E. (2005). Importance of the diazotrophs as a source of new nitrogen in the ocean. *J Sea Res* **53**: 67–91.

Luo YW, Doney SC, Anderson LA, Benavides M, Bode A, Bonnet S *et al.* (2012). Database of diazotrophs in global ocean: abundances, biomass and nitrogen fixation rates. *Earth Syst Sci Data* **5**: 47–106.

Mills MM, Ridame C, Davey M, La Roche J, Geider RJ. (2004). Iron and phosphorus co – limit nitrogen fixation in the eastern tropical North Atlantic. *Nature* **429**: 292–294.

Mohr W, Großkopf T, Wallace DWR, LaRoche J. (2010a). Methodological underestimation of oceanic nitrogen fixation rates. *PLoS One* **5**: e12583.

Mohr W, Intermaggio MP, LaRoche J. (2010b). Diel rhythm of nitrogen and carbon metabolism in the unicellular, diazotrophic cyanobacterium *Crocosphaera watsonii* WH8501. *Environ Microbiol* **12**: 412–421.

Moisander PH, Beinart RA, Hewson I, White AE, Johnson KS, Carlson CA *et al.* (2010). Unicellular cyanobacterial

distributions broaden the oceanic N_2 fixation domain. *Science* **327**: 1512–1514.

Montoya JP, Holl CM, Zehr JP, Hansen A, Villareal TA, Capone DG. (2004). High rates of N_2 fixation by unicellular diazotrophs in the oligotrophic Pacific Ocean. *Nature* **430**: 1027–1032.

Montoya JP, Voss M, Kahler P, Capone DG. (1996). A simple, high-precision, high-sensitivity tracer assay for N_2-fixation. *Appl Environ Microbiol* **62**: 986–993.

Musat N, Stryhanyuk H, Bombach P, Adrian L, Audinot J-N, Richnow HH. (2014). The effect of FISH and CARD-FISH on the isotopic composition of ^{13}C and ^{15}N-labeled *Pseudomonas putida* cells measured by nanoSIMS. *Syst Appl Microbiol* **37**: 267–276.

Pernthaler A, Amann R. (2004). Simultaneous fluorescence in situ hybridization of mRNA and rRNA in environmental bacteria. *Appl Environ Microbiol* **70**: 5426–5433.

Pernthaler A, Pernthaler J, Amann R. (2004). Sensitive multi-color fluorescence in situ hybridization for the identification of environmental microorganisms. *Mol Microb Ecol Man* **3**: 711–726.

Ploug H, Musat N, Adam B, Moraru CL, Lavik G, Vagner T *et al.* (2010). Carbon and nitrogen fluxes associated with the cyanobacterium *Aphanizomenon* sp. in the Baltic Sea. *ISME J* **4**: 1215–1223.

Polerecky L, Adam B, Milucka J, Musat N, Vagner T, Kuypers MMM. (2012). Look@NanoSIMS–a tool for the analysis of nanoSIMS data in environmental microbiology. *Environ Microbiol* **4**: 1009–1023.

Rees AP, Gilbert JA, Kelly – Gerreyn BA. (2009). Nitrogen fixation in the western English Channel (NE Atlantic ocean). *Mar Ecol Prog Ser* **374**: 7–12.

Ridame C, Guieu C. (2002). Saharan input of phosphate to the oligotrophic water of the open western Mediterranean Sea. *Limnol Oceanogr* **47**: 856–869.

Sañudo-Wilhelmy SA, Kustka AB, Gobler CJ, Hutchins DA, Yang M, Lwiza K *et al.* (2001). Phosphorus limitation of nitrogen fixation by *Trichodesmium* in the central Atlantic Ocean. *Nature* **411**: 66–69.

Shi T, Sun Y, Falkowski PG. (2007). Effects of iron limitation on the expression of metabolic genes in the marine cyanobacterium *Trichodesmium erythraeum* IMS101. *Environ Microbiol* **9**: 2945–2956.

Short SM, Zehr JP. (2007). Nitrogenase gene expression in the Chesapeake Bay Estuary. *Environ Microbiol* **9**: 1591–1596.

Simon N, Campbell L, Örnólfsdóttir E, Groben R, Guillou L, Lange M *et al.* (2000). Oligonucleotide probes for the identification of three algal groups by dot blot and fluorescent whole-cell hybridization. *J Eukaryot Microbiol* **47**: 76–84.

Sohm JA, Webb EA, Capone DG. (2011). Emerging patterns of marine nitrogen fixation. *Nat Rev Microbiol* **9**: 499–508.

Strathmann RR. (1967). Estimating the organic carbon content of phytoplankton from cell volume or plasma volume. *Limnol Oceanogr* **12**: 411–418.

Thompson A, Carter BJ, Turk-Kubo K, Malfatti F, Azam F, Zehr JP. (2014). Genetic diversity of the unicellular nitrogen-fixing cyanobacteria UCYN-A and its prymnesiophyte host. *Environ Microbiol* **16**: 3238–3249.

Thompson AW, Foster RA, Krupke A, Carter BJ, Musat N, Vaulot D *et al.* (2012). Unicellular cyanobacterium symbiotic with a single-celled eukaryotic alga. *Science* **337**: 1546–1550.

Tripp HJ, Bench SR, Turk KA, Foster RA, Desany BA, Niazi F *et al.* (2010). Metabolic streamlining in an open-ocean nitrogen-fixing cyanobacterium. *Nature* **464**: 90–94.

Tuit C, Waterbury J, Ravizza G. (2004). Diel variation of molybdenum and iron in marine diazotrophic cyanobacteria. *Limnol Oceanogr* **49**: 978–990.

Turk-Kubo KA, Achilles KM, Serros TR, Ochiai M, Montoya JP, Zehr JP. (2012). Nitrogenase (nifH) gene expression in diazotrophic cyanobacteria in the Tropical North Atlantic in response to nutrient amendments. *Front Aquat Microbiol* **3**: 386.

Verity PG, Robertson CY, Tronzo CR, Andrews MG, Nelson JR, Sieracki ME. (1992). Relationships between cell volume and the carbon and nitrogen content of marine photosynthetic nanoplankton. *Limnol Oceanogr* **37**: 1434–1446.

Villareal TA. (1991). Nitrogen-fixation by the cyanobacterial symbiont of the diatom genus *Hemiaulus*. *Mar Ecol Prog Ser* **76**: 201–204.

Voss M, Croot P, Lochte K, Mills M, Peeken I. (2004). Patterns of nitrogen fixation along 10 °N in the tropical Atlantic. *Geophys Res Lett* **31**: 1–4.

Wallner G, Amann R, Beisker W. (1993). Optimizing fluorescent in situ hybridization with rRNA targeted oligonucleotide probes for flow cytometric identification of microorganisms. *Cytometry* **14**: 136–143.

Wilson ST, Böttjer D, Church MJ, Karl DM. (2012). Comparative assessment of nitrogen fixation methodologies conductedin the oligotrophic North Pacific Ocean. *Appl Environ Microbiol* **78**: 6516–6523.

Zani S, Mellon MT, Collier JL, Zehr JP. (2000). Expression of *nifH* genes in natural microbial assemblages in Lake George, New York, detected by reverse transcriptase PCR. *Appl Environ Microbiol* **66**: 3119–3124.

Zehr JP, Bench SR, Carter BJ, Hewson I, Niazi F, Shi T *et al.* (2008). Globally distributed uncultivated oceanic N_2-fixing cyanobacteria lack oxygenic photosystem II. *Science* **322**: 1110–1112.

Zehr JP, McReynolds LA. (1989). Use of degenerate oligonucleotides for amplification of the *nifH* gene from the marine cyanobacterium *Trichodesmium thiebautii*. *Appl Environ Microbiol* **55**: 2522–2526.

Zehr JP, Mellon MT, Zani S. (1998). New nitrogen-fixing microorganisms detected in oligotrophic oceans by amplification of nitrogenase (*nifH*) genes. *Appl Environ Microbiol* **64**: 3444–3450.

Zehr JP, Waterbury JB, Turner PJ, Montoya JP, Omoregie E, Steward GF *et al.* (2001). Unicellular cyanobacteria fix N_2 in the subtropical North Pacific Ocean. *Nature* **412**: 635–637.

Supplementary Information accompanies this paper on The ISME Journal website (http://www.nature.com/ismej)